Available online at www.sciencedirect.com
ScienceDirect
Journal of Hazardous Materials 157 (2008) 8–17
Journal of Hazardous Materials
www.elsevier.com/locate/jhazmat

Modeling the effect of pH on biosorption of heavy metals by citrus peels

Silke Schiewer*, Santosh B. Patil

Department of Civil & Environmental Engineering, University of Alaska Fairbanks, PO Box 755900, Fairbanks, AK 99775, USA

Received 11 July 2007; received in revised form 22 November 2007; accepted 19 December 2007
Available online 28 December 2007

Abstract

Biosorption by materials such as citrus peels could be a cost effective technique for removing toxic heavy metals from wastewater. Orange peels, lemon peels and lemon-based protonated pectin peels (PPP) had Langmuir sorption capacities of 0.7–1.2 mequiv./g (39–67 mg/g) of Cd per biosorbent dry weight. A potentiometric titration was interpreted using a continuous pK_a spectrum approach. It revealed four acidic sites with pK_a values of 3.8, 6.4, 8.4 and 10.7, and a total site quantity of 1.14 mequiv./g. Sorption isotherms of untreated citrus peels showed an unusual shape with two plateau values. Protonated pectin peels on the other hand showed a typical Langmuir behavior with a higher sorption capacity than untreated peels. At lower pH, metal binding was reduced due to increased competition by protons. This was modeled using pH-sensitive isotherm equations. It was not necessary to assume four binding sites; using one site with pK_a 3.8 and a quantity of 1.14 mequiv./g was sufficient. It was possible to accurately predict metal uptake at one pH using the metal binding constant determined at a different pH. A 1:1 stoichiometry model fit the sorption isotherms shape better than a 1:2 stoichiometry. For constant pH, the 1:1 stoichiometry reduces to the Langmuir model.

Keywords: Biosorption; Cadmium; Citrus peels; Isotherm; pK_a spectrum

1. Introduction

The discharge of toxic heavy metals into the environment from industrial activities such as mining and metal processing can lead to numerous environmental problems. Therefore, it is important to remove heavy metals from waste streams. Conventional metal removal techniques such as ion exchange or precipitation are often either expensive or not sufficiently effective in the low concentration range. Biosorption, the passive uptake of pollutants such as heavy metals by biological materials, can be both highly efficient and cost effective. Low cost sorbents with high metal binding need to be investigated. Using waste materials from agriculture and food industries as biosorbents has the dual advantage of waste reuse and low sorbent cost. The question arises, which wastes are good sorbents. The high metal binding capacity of biosorbents like brown algae has been attributed to carboxylate groups of cell wall polysaccharides like alginate [1–3]. Therefore, one should investigate waste materials containing large amounts of polysaccharides with acidic functional groups.

1.1. Biosorption by pectin-rich sorbents

Fruit waste materials are typically generated in large quantities by the fruit juice industry. These materials have received little scientific attention, in spite of their high quantity of pectin, which contains carboxylate groups. The plant cell wall polysaccharide pectin consists mostly of polygalacturonic acid, which is partially esterified with methyl groups. Pectin polymers with a low degree of esterification (low methoxyl pectin) can cross-link through calcium bridging between two deprotonated carboxylate groups. This leads to the formation of gels widely used in the food industry. Commercial pectin is extracted from citrus peels and apple residues.

Dronnet et al. found that acetyl groups, which are common in sugar beet pectin, are responsible for a lower metal binding affinity of sugar beet pectin compared to citrus peel pectin. Citrus peels typically have a lower degree of acetylation [4]. According to Renard and Jarvis [5], acetylation and methylation of pectin decreases the affinity for heavy metals, with different binding mechanisms involved for strongly bound Pb and weakly bound Ca. For sugar beet pulp, metal binding occurred faster at higher pH values, and the equilibrium could be described by Langmuir isotherms [6]. In potentiometric titrations of sugar beet pulp, carboxylate groups with pK_a 3.7 and pK_a 4.8, as

* Corresponding author. Tel.: +1 907 474 2620; fax: +1 907 474 6087.
E-mail address: ffsos@uaf.edu (S. Schiewer).

0304-3894/$ – see front matter © 2007 Elsevier B.V. All rights reserved.
doi:10.1016/j.jhazmat.2007.12.076

well as a weakly acidic (likely phenolic) group were identified [7].

Very little information is available on biosorption performance of other pectin-rich materials, such as residues from fruit juice production, orange peels, apple residues, or other kinds of fruit peels [8–13], or pectin itself [14–16]. A recent review of low cost biosorbents highlighted the abundance of studies on seaweeds compare to fewer studies focusing on agricultural/food byproducts. Among the latter, broad been peels, orange peels, and pea peels had high Cd binding capacities, exceeding 1 mmol/g [17]. Simple Langmuir and Freundlich isotherms, which cannot describe pH effects, were used to describe metal binding by citrus peels [9,18–20] as well as orange and banana peels [12]. Perez Marin [21] found that the Sips model fit better than the Langmuir isotherm which in turn fit better than the Freundlich isotherm. This is not surprising since the Sips model resembles the Langmuir model except for having one more adjustable parameter. So far, models presented in published studies of metal binding by citrus peels have not taken pH effects into account. However, it has been observed that sorption of metals such as Cd and Pb by untreated or chemically modified orange peels increases with pH up to about pH 5 or 6. At higher pH, a decrease in metal uptake was observed due to metal hydrolysis [19–21]. Therefore one of the goals of the present work is to describe metal binding by citrus peels with a pH-sensitive model. To make this model mechanistically based, site quantities and pK_a values for the model were derived from pH titrations.

1.2. Titration data processing

For biosorbents with acidic functional groups, the sorbent surface charge changes with pH. This change in surface charge with pH can be described by resolving titration curves with discrete or continuous pK_a spectra. To determine the acidity constants for a given number of discrete sites, the classical least-square method can be used. However, the solution is dependent on the assumed number of binding sites and may be unstable [22]. To circumvent these difficulties, Smith and Ferris [23] developed a fully optimized continuous (FOCUS) pK_a spectrum technique to fit acid–base titration data and to evaluate binding site acidity constants. This method, which involves additional non-negativity constraints and regularizing functions, is advantageous because it simultaneously optimizes the smoothness of the pK_a spectrum and the fit. While it is easier to derive a discrete model with a limited number of acidic sites, the continuous spectrum technique yields a stable solution and provides binding site concentrations as well as corresponding pK_a without requiring predetermination of the number or pK_a of binding sites.

1.3. Equilibrium modeling

Modeling equilibrium sorption is important for industrial applications of biosorption; it yields data that facilitates designing and optimizing the process. The classical Langmuir and Freundlich sorption isotherm models consider sorption by free binding sites rather than ion exchange. Nevertheless, these isotherm models are still widely used for modeling the biosorption equilibrium because of their simplicity. The alternative ion exchange modeling approach, assumes that other ions, such as calcium, are replaced by metal ions. However, ion exchange constants do not account for variable cation exchange capacity. The number of available sites can vary with pH due to protonation–deprotonation of weakly acidic sites. At constant pH, modeling with ion exchange constants can yield behavior similar to that of a Langmuir isotherm, since the ratio of proton-occupied and free sites is constant at constant pH.

A biosorption equilibrium model based on a more realistic combination of ion exchange and acid/base reactions was developed by Schiewer and Volesky [3]. This pH-sensitive model considers ion exchange between metal ions and protons as well as binding to already unprotonated sites. For divalent ions, a 1:2 stoichiometry was applicable, where one metal ion binds to two monoprotic sites. The pH-sensitive model takes into account that binding of the displaced ion (proton) is a reversible reaction. Another major advantage to this model is that the effect of pH on metal binding can actually be predicted using the same metal binding constants for different pH values.

2. Materials and methods

2.1. Biomass preparation

Three types of citrus materials were compared: native orange peels, native lemon peels, and lemon-based "pectin peels" obtained from Sunkist®. The first part of the experiments focused on a comparison between citrus species (native orange and lemon peels obtained from a local grocery store), the second part of the experiments used a partially processed lemon peel product, "pectin peels", provided by Sunkist®. Data for the latter lemon-based product were compared with native lemon peels to evaluate the effect of peel processing on sorption performance.

The lemon and orange peels were washed three times with nano-pure water (approximately 18 Ω resistance), dried at 38–40 °C in a convection oven for 12 h, ground, and screened.

Sunkist® provided this project with a material they term "pectin peels". Those are produced from juice manufacturing residues by leaching of the soluble sugars and drying. According to Sunkist®, the moisture content was approximately 10% and the pectin content 28%. This material was protonated to remove excess cations such as calcium or sodium that could interfere with metal sorption and to create a more defined sorbent material [3]. After washing three times (as described above), the sample was treated with 0.1N HNO_3 for 6 h, dried for 12 h at 38–40 °C, washed again three times with nano-pure water to remove excess acid or remaining ions, dried, ground and sieved. The resulting material is referred to as protonated pectin peels (PPP).

2.2. Potentiometric titration for determining acid/base properties

Acid–base titrations were used to investigate the chemical nature and concentration of reactive sites of the sorbent. The weighed protonated lemon waste (0.5 g) of 0.7–0.9 mm diam-

eter was immersed in 50 mL of nano-pure water for 2 h and agitated with a magnetic stir bar at 120 rpm. Nitrogen gas was continuously bubbled through the solution to avoid carbonic acid formation. Volume increments of 0.05 mL of 0.071N NaOH were added to the reaction flask after 3–7 min of equilibration and the corresponding changes in pH were noted, until pH reached 11.05. The same procedure was repeated for a blank titration. Based on the experimental data, the total charge after the ith addition of titrant is expressed as

$$S_{\mathrm{exp},i} = \frac{[\mathrm{Na}^+]_i + [\mathrm{H}^+]_i - [\mathrm{OH}^-]_i}{m/V} \quad (1)$$

where $S_{\mathrm{exp},i}$ is the experimentally determined charge (mequiv./g); $[\mathrm{Na}^+]_i$, $[\mathrm{H}^+]_i$ and $[\mathrm{OH}^-]_i$ are the concentration of sodium resulting from the addition of base, the proton, and the hydroxyl concentrations (mol/L), respectively, in the solution; and m/V is the biosorbent mass m (g) per solution volume V (L).

2.3. Titration data processing with a continuous pK_a spectrum

The fully optimized continuous (FOCUS) pK_a spectrum technique developed by Smith and Ferris [23] was used here. The total charge is the sum of charges of m different sites, which are assumed to be monoprotic. For the jth site with dissociation constant K_{aj} the following equations apply:

$$[\mathrm{H}^+] + [\mathrm{B}_j{}^-] \leftrightarrow [\mathrm{BH}_j] \quad (2)$$

$$K_{aj} = \frac{[\mathrm{H}^+][\mathrm{B}_j{}^-]}{[\mathrm{BH}_j]} \quad (3)$$

$$[B_{\mathrm{T}j}] = [\mathrm{B}_j{}^-] + [\mathrm{BH}_j] \quad (4)$$

The total site concentration ($B_{\mathrm{T}j}$) consists of the free binding site concentration ($\mathrm{B}_j{}^-$) and the protonated binding site concentration (BH_j) (mol/L). The charge can be calculated by combining Eqs. (3) and (4) for all m sites:

$$S_{\mathrm{cal},i} = \sum_{j=1}^{m} \left(\frac{B_{\mathrm{T}j} K_{aj}}{K_{aj} + [\mathrm{H}^+]_i} \right) + S_0 \quad (5)$$

The term S_0 is added in order to account for any initial charge on the surface. To fit the model (Eq. (5)) to the experimental data (Eq. (1)), a sequence of closely spaced pK_a values (2, 2.2, …, 11, 11.2) were fixed, and initial concentrations for the quantity of each site were randomly assigned. Eq. (5) is transformed as

$$S = AB \quad (6)$$

$$A(i,j) = \frac{K_{a\,j}}{K_{a\,j} + [\mathrm{H}^+]_i} \quad \text{for } i = 1 \ldots n \quad \text{and} \quad j = 1 \ldots m \quad (7)$$

where A is an $n \times (m+1)$ matrix, which represents the degree of dissociation; B is an $(m+1) \times 1$ vector of unknown total site concentrations ($B_{\mathrm{T}j}$); and S is an $n \times 1$ vector of charge (n: total number of titration data points, m: total number of binding sites). Eq. (6) was solved by using Matlab®-Optimization toolbox (The Math Works Inc.). This is an ill-posed problem, because it does not yield a unique solution. We adopted an approach proposed by Cernik et al. [22], imposing the constraint that site concentrations are not negative. The outcome was smoothed by regularized least-squares optimization, minimizing the term $SS + \lambda R$, with the sum of square deviations

$$SS = \sum_{i=1}^{m} (S_{\mathrm{cal},i} - S_{\mathrm{exp},i})^2 \quad \text{with } S \geq 0 \quad (8)$$

and the regularization parameter

$$R = \sum_{j=2}^{m-1} (\mathrm{B}_{j-1} - 2\mathrm{B}_j + \mathrm{B}_{j+1})^2 \quad (9)$$

According to Cernik et al. [22], R is small for smooth affinity distributions and large for strongly oscillating functions. The solution depends on the regularization strength parameter λ, which is varied from $\lambda = 0$ for a total of k different values.

2.4. Isotherm experiments

For these experiments, 0.1 g of sorbent (particle size 0.7–0.9 mm) were contacted with a synthetic solution of $CdCl_2$ (initial concentration of 10–700 mg/L) on an orbital shaker for 6 h. Prior experiments had shown that equilibrium was achieved in about 1 h [18]. The pH was maintained constant at either 5.0 or 3.0 throughout the experiment by adding 0.1N NaOH or HCl. Blank tests (without biosorbent) were performed to confirm that metal precipitation or adsorption did not interfere with biosorption. The resulting suspension of metal solution and biosorbent material was filtered, and the concentration of metal in the liquid phase was determined by AAS (PerkinElmer AAnalyst 300). The metal uptake per gram of biosorbent material was determined using the mass balance. If C_0 and C_e are the initial and final metal concentrations (mequiv./L), respectively, V is the suspension volume (L) and m is the mass of biosorbent material (g), then the equilibrium metal uptake q_e (mg/g or mequiv./g) can be calculated as

$$q_e = \frac{V(C_0 - C_e)}{m} \quad (10)$$

The results were plotted as sorption isotherms of the sorbate uptake (q_e) versus the equilibrium concentration of the residual sorbate remaining in the solution (C_e).

2.5. Sequential additions method

For further equilibrium studies, the sequential additions method SAM [24] was used. If individual flasks are used for each data point, variations between points of an isotherm can occur due to possible biomass heterogeneity. The SAM eliminates this cause of data scattering. First, 0.1 g of the citrus peel was suspended in 50 mL nano-pure water. For each of i additional steps, a small volume v_i (L) of concentrated $Cd(NO_3)_2$ solution of known concentration C_c (mequiv./L) was added to the suspen-

sion, thus gradually increasing the Cd concentration. Magnetic stirring agitated the suspension for the required equilibration time of 60 min [18]. The pH was maintained at 5.0 by adding 0.01 or 0.1N NaOH. Next, a suspension volume $u = 1.5$ mL was removed, filtered using Whatman 40 ashless filter paper, and the metal concentration in the filtrate C_i was analyzed by AAS. The above steps of metal addition, equilibration and sampling were repeated until the desired maximum metal concentration was reached. The equilibrium uptake q_i after each ith step was calculated using the mass balance (Eq. (11)), taking into account the amount of metal added and removed in all prior steps and the corresponding increase in total solution volume V_i (L), as well as the decrease in sorbent mass m_i (g) in solution.

$$C_c v_i + C_{i-1}(V_{i-1} - u) + q_{i-1}m_{i-1} = C_i V_i + q_i m_i \quad (11)$$

$$V_i = V_{i-1} - u + v_i \quad (12)$$

$$m_i = m_{i-1}\left(\frac{1-u}{V_{i-1}}\right) \quad (13)$$

2.6. Langmuir isotherm model

The Langmuir isotherm, one of the most ubiquitous models used to describe the relationship between equilibrium metal uptake (q_e) and final concentrations (C_e), is given as

$$q_e = \frac{Kq_{max}C_e}{(1 + KC_e)} \quad (14)$$

K (L/mequiv.) is the equilibrium adsorption constant which is related to the affinity of the binding sites. The term q_{max} (mequiv./L) is the maximum amount of metal ions bound per unit mass of biosorbent when all binding sites are occupied. The Langmuir parameters can be determined from a linearized form of Eq. (14) (by plotting C_e/q_e vs. C_e):

$$\frac{C_e}{q_e} = \frac{1}{Kq_{max}} + \frac{C_e}{q_{max}} \quad (15)$$

To determine the model fit, root mean squared errors (RMSE) were calculated: the squared difference between the experimental metal uptake data (q) and the corresponding model predictions for the uptake (q_m) were summed up. This sum was then divided by the number of data points (p) for each data set to calculate the mean square error. After taking the root of that term, the RMSE is obtained. The RMSE can be considered as the average deviation between the predicted uptake and the actual uptake.

$$\mathrm{RMSE} = \sqrt{\frac{\sum_1^p (q - q_m)^2}{p}} \quad (16)$$

2.7. Modeling equilibrium with pH-sensitive isotherm

Schiewer and Volesky [3] developed a model for binding of divalent metal ions by monovalent acidic sites. This model is based on a combination of ion exchange and acid/base reactions. The pH-sensitive isotherm model, which assumes a 1:2 stoichiometry, where one divalent metal ion M^{2+} binds to two monovalent binding sites B, was derived from the following equations:

$$M^{2+} + 2B^- \leftrightarrow 2BM_{0.5} \quad (17)$$

$$K_a = \frac{[H]B^-}{BH}\ (\mathrm{mol/L}) \quad (18)$$

$$K_{BM}\frac{BM_{0.5}^2}{C_e B^2}\ (\mathrm{L/mmol}) \quad (19)$$

$$B_T = B^- + BH + BM_{0.5}\ (\mathrm{mequiv./g}) \quad (20)$$

whereby C_e is the concentration of a divalent metal ion M^{2+}, which forms a complex $BM_{0.5}$ with an acidic site B with the metal binding constant K_{BM}. Combining Eqs. (18)–(20) yields Eq. (21):

$$q_M = BM_{0.5} = \frac{B_T(K_{BM}C_e)^{0.5}}{1 + [H^+]/K_a + (K_{BM}C_e)^{0.5}}\ (\mathrm{mequiv./g}) \quad (21)$$

As an alternative to the above equations for 1:2 stoichiometry, consider the following approach for a 1:1 binding stoichiometry:

$$M + B^- \leftrightarrow BM \quad (22)$$

$$K_{BM} = \frac{BM}{C_e B^-}\ (\mathrm{L/mmol}) \quad (23)$$

$$B_T = B^- + BH + BM\ (\mathrm{mequiv./g}) \quad (24)$$

From Eqs. (18), (23) and (24), the following isotherm expression can be derived.

$$q_M = BM = \frac{B_T K_{BM} C_e}{1 + [H^+]/K_a + K_{BM}C_e}\ (\mathrm{mequiv./g}) \quad (25)$$

Both approaches (1:2 and 1:1 stoichiometries) were used to fit the data obtained through the subsequent additions method at pH 3 and pH 5 for protonated lemon waste. Optimal model parameters were obtained by minimizing the RMSE. In some cases, the number of sites B_T was optimized; in others, the total number of sites as determined by titration was used for B_T. In either case, the acid dissociation constant was obtained from titration. A major advantage of both model versions is that the effect of pH on metal binding can actually be predicted. Though the 1:2 stoichiometry appears intuitively more appropriate for divalent metals from a mechanistic standpoint, the 1:1 stoichiometry was also considered.

For constant pH, where the term $(1 + [H^+]/K_a)$ is constant, isotherm Eq. (25) for 1:1 stoichiometry can be reduced to the Langmuir isotherm Eq. (14), where $K_{BM}/(1 + [H^+]/K_a)$ corresponds to the Langmuir constant K, and $[B_T]$ corresponds to q_{max}:

$$q_M = BM = \frac{B_T(K_{BM}/(1 + [H^+]/K_a))C_e}{1 + (K_{BM}/(1 + [H^+]/K_a))C_e} = \frac{q_{max}KC_e}{1 + KC_e} \quad (26)$$

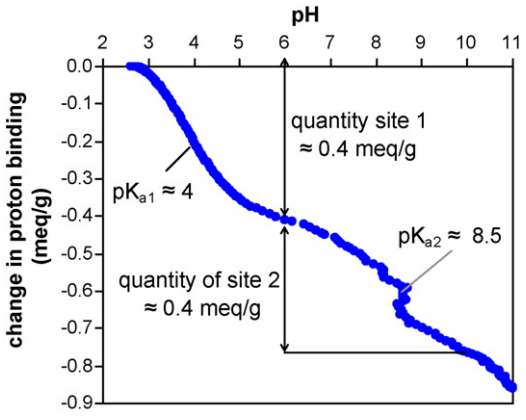

Fig. 1. Potentiometric titration of protonated pectin peels.

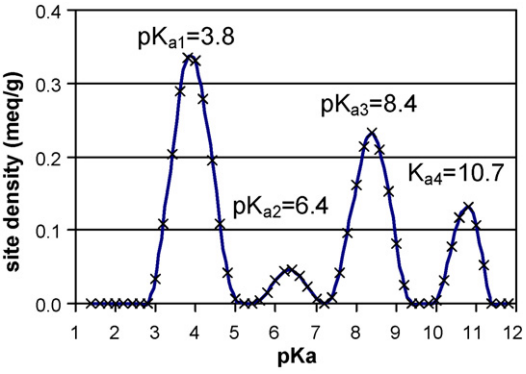

Fig. 2. Regularized pK_a spectrum of protonated pectin peels based on data of Fig. 1.

3. Results and discussion

3.1. Potentiometric titration

The change in proton binding versus pH, as calculated from a proton mass balance, is shown in Fig. 1. The presence of inflections around pH 4 and 8.5 was evident, providing a first indication of binding sites on the biosorbent material. Carboxylate groups typically have pK_a values between 3 and 5 [25]. Due to the high pectin content of citrus peels, carboxylate groups are likely one of the prominent groups present and responsible for the inflection around pH 4.

A more thorough analysis of the pK_a values was performed through the FOCUS technique with regularization [23], which resulted in the continuous pK_a spectrum represented in Fig. 2. Four sites were identified as distinct peaks. The area under each peak corresponds to the site concentration. The site concentrations and pK_a values appear in Table 1.

The total site concentration (sum of all sites) was 1.14 mequiv./g. This includes the initial value of 0.2 mequiv./g for negatively charged sites already present at the beginning of the titration (pH 2.6), before any base was added. This initial charge is due to the presence of sites with a lower pK_a value, one that does not fall within the titrated pH range. The two main sites, with quantities of 0.39 and 0.27 mmol/g (together they represent 60% of the total sites), had pK_a values of 3.8 and 8.4, respectively. These values correspond well to the observable inflections in Fig. 1. The pK_{a1} = 3.8 could be attributed to presence of carboxylate groups in lemon fruit waste. Since citrus peels are rich in pectin, it is only to be expected that carboxylate groups are one of the main functional groups in citrus peels. According to studies by Lee et al. [10] and Reddad et al. [7], phenolic functional groups could correspond to the higher pK_a, while phosphate groups could be responsible for one of the intermediate pK_a values.

Table 1
Site concentrations with corresponding pK_a values determined from pK_a spectrum

Site	Concentration B_T (mequiv./g)	pK_a
Initial base value	0.20	<2
Site 1	0.39	3.8
Site 2	0.11	6.4
Site 3	0.27	8.4
Site 4	0.17	10.7
Total	1.14	

The site concentrations and pK_a values listed in Table 1 are further validated by comparing the modeled charge (solid line) with experimental values (symbols) in Fig. 3. Experimental titration data were evaluated according to Eq. (1) to calculate the charge excess. Fig. 3 depicts the absolute magnitude of the negative charge. A very good fit can be observed. The dashed lines represent the contributions of the individual groups to the total charge. It is apparent that up to approximately pH 6, Site 1 (carboxylate) and the initial charge dominate the total charge. All model predictions shown in Fig. 2 are assuming four discrete sites with properties as listed in Table 1 (though the site quantities and pK_a values were obtained from a continuous pK_a spectrum to obtain more reliable values), showing that a simpler multi-site discrete model is sufficient.

3.2. Two-stage metal binding isotherms

The sorption isotherm data in Fig. 4 show an unusual two-stage shape with two plateaus. This behavior is not compatible

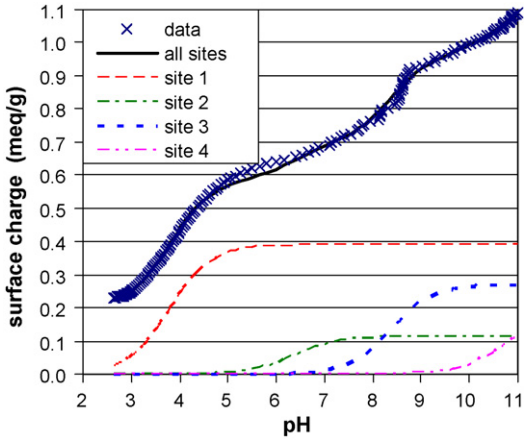

Fig. 3. Comparison between surface charge experimental data and predictions of four site model, including contribution of individual sites to the surface charge.

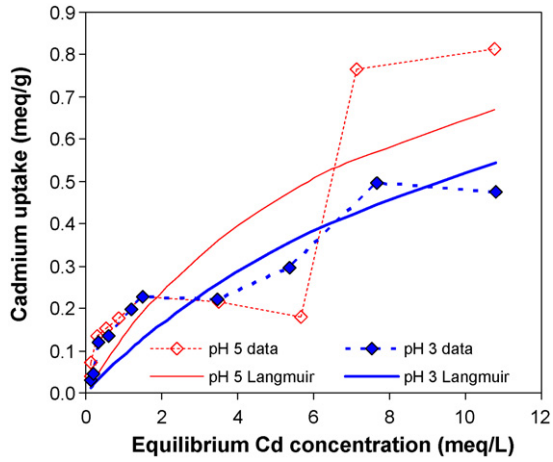

Fig. 4. Sorption isotherms for cadmium binding to untreated orange peels at pH 3 and pH 5. Experimental data connected by dashed lines and Langmuir modeling with nonlinear optimization of K assuming q_{max} = 1.14 mequiv./g.

with classical Langmuir or Freundlich isotherms. Assuming q_{max} as equal to the total number of binding sites determined for PPP by titration (see Table 1), the Langmuir parameter K was optimized to minimize RMSE. The model predictions shown as solid lines in Fig. 4 clearly did not fit the experimental data. Using other approaches for parameter determination, such as linearization or simultaneous nonlinear optimization of q_{max} and K, did not lead to a notably better fit (see Table 2). Using the total number of binding sites as determined by titration of PPP for q_{max} has the advantage of ensuring a realistic number of binding sites (which was otherwise not the case for orange peels at pH 5) and allowing an easier comparison between different materials, since K is the only parameter that varies for different pH values or materials.

The anomalous two-stage-shape behavior (more pronounced for orange peels than for lemon peels) could have been due to a combination of the following factors:

1. Heterogeneity of biosorbent material (e.g. inner peel vs. outer peel) at different equilibrium points; that is, "scattering" of data. Since each data point was obtained from an individual experiment, the sorbent properties could have differed between flasks.
2. Formation of cationic metal complexes (e.g. $CdCl^+$) which compete with cadmium ions to sorb on the citrus peels. At pH 5, free Cd^{2+} ranged between 98% and 54% of the total cadmium for a Cd concentration range of 0.1–10 mM, while that of $CdCl^+$ increased from 2% to 44% according to predictions of the chemical equilibrium program MINTEQ. The speciation at pH 3 is very similar to that at pH 5 since metal hydroxide species are negligible.
3. Two binding sites with different affinities for cadmium ions. The binding site with the strongest affinity for Cd^{2+} became saturated at the first plateau, then cadmium ions bound to a less favored binding site.
4. Conformational changes in the polygalacturonate gel, whereby increasing Cd^{2+} binding changes the pectin gel structure from a less ordered state to an ordered form. Such an ordered configuration has been described by Grant et al. [26] as the "egg box" model, for the gel structure in the presence of ions like calcium. The ordered gel structure could facilitate binding of additional Cd^{2+} ions by providing suitable "pockets" with the right spatial configuration for Cd^{2+} binding.

To determine which of the above factors were responsible for the anomalous behavior, the following changes were made to the experimental procedure:

Table 2
Summary of Langmuir isotherm model parameters

Biosorbent material	Parameters obtained by linearization[a]				Parameters obtained by minimizing RMSE			
	K (L/mequiv.)	q_{max} (mequiv./g)	R^2	RMSE	K (L/mequiv.)	q_{max} (mequiv./g)	RMSE	Fig
pH 3								
Orange peels, $CdCl_2$	0.40	0.55	0.88	0.053	0.37	0.57	0.053	4
					0.084	**1.14**[b]	**0.067**	
Lemon peels, $CdCl_2$	0.46	0.71	0.97	0.041	0.53	0.68	0.040	–
					0.15	1.14[b]	0.074	
PPP, SAM, $Cd(NO_3)_2$	0.50	0.86	0.90	0.035	0.51	0.88	0.033	6
					0.30	1.14[b]	0.047	
pH 5								
Orange peels, $CdCl_2$	0.31	0.67	0.35	0.16	0.0027[c]	30.0[c]	0.13	4
					0.13	**1.14**[b]	**0.143**	
Lemon peels, $CdCl_2$	0.35	0.93	0.88	0.076	**0.33**	**1.00**	**0.074**	5
					0.24	1.14[b]	0.077	
PPP, $CdCl_2$	3.80	1.01	0.96	0.105	**1.77**	**1.11**	**0.081**	5
					1.63	1.14[b]	0.081	
PPP, SAM, $Cd(NO_3)_2$	1.58	1.19	0.97	0.048	**1.95**	**1.19**	**0.031**	5, 6
					2.16	1.14[b]	0.034	

Bold values are parameters used for model predictions shown in Figs. 4 and 5.

[a] Values for orange and lemon peels as earlier reported [18].

[b] Utilizing site quantity q_{max} as determined in titration of PPP, only optimizing K.

[c] Model predicts straight line: parameters K and q_{max} could not be determined independently.

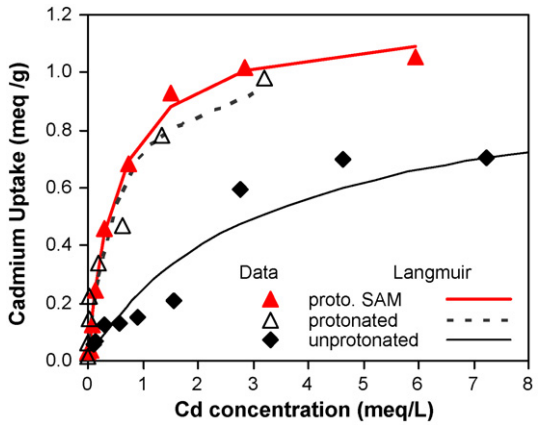

Fig. 5. Comparison of sorption isotherms for protonated pectin peels (using $CdNO_3$ and the SAM method) as well as protonated pectin peels and non-protonated lemon peels (both using $CdCl_2$ and the conventional experimental method). Experimental data and Langmuir modeling with nonlinear parameter optimization of both K and q_{max}.

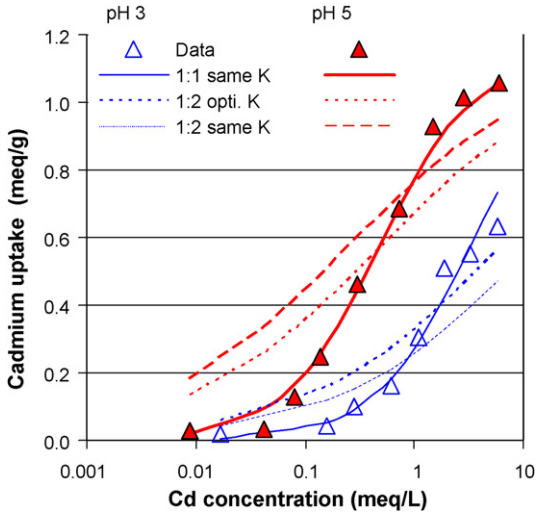

Fig. 6. Comparison of sorption isotherms for protonated pectin peels (PPP) at pH 5 and pH 3, using $Cd(NO_3)_2$ and the SAM method. Experimental data and pH-sensitive ion exchange models for 1:1 and 1:2 stoichiometry. The parameter K was either optimized for the respective pH value ("opti K") or the same K value was fitted for both pH values ("same K") for an actual prediction of the effect of pH.

1. Isotherm studies were carried out using SAM [24] to eliminate the effect of biosorbent heterogeneity on the equilibrium data.
2. Cadmium chloride salt was replaced by cadmium nitrate salt, since nitrate is not expected to form significant quantities of complexes with cadmium.
3. A better-defined sorbent material, protonated pectin peels (PPP), was used. Due to prior processing, this material is low in impurities, with few cations other than protons and higher pectin content.

Fig. 5 shows the results of equilibrium experiments using the conventional method and $CdCl_2$ salt solution, compared to using SAM and $Cd(NO_3)_2$. When protonated pectin peels were used, very similar results were obtained, regardless of the type of salt or experimental method used ($CdCl_2$ and conventional method vs. $CdNO_3$ and SAM, Fig. 5). The type of anions used (Cl^- or NO_3^-) apparently had very little effect on metal binding, which makes it unlikely that sorption of $CdCl^+$ complexes was responsible for the two-stage isotherm. Similarly, the experimental methodology (SAM or conventional) did not affect the results, which means data scattering due to sorbent sample heterogeneity can be ruled out as a cause for the unusual isotherm. For further experiments, the SAM was used since it was less time consuming and more controllable than the conventional experimental procedure, and the effect of sorbent heterogeneity was completely removed.

The main factor responsible for the two-stage isotherms appears to have been the sorbent material. While two-stage isotherms were observed in untreated lemon peels (see Fig. 5), "normal" isotherms were observed for protonated pectin peels in both cases (conventional method and SAM, Fig. 5). These observations suggest that the processing of the pectin peels (leaching of soluble components performed by the manufacturer, followed by protonation performed by the investigators) decreased heterogeneity of the biosorbent materials. The anomalous behavior may have been due to involvement of several binding sites in cadmium binding. However, additional research is necessary to compare binding sites in treated and untreated lemon peels. As shown in Figs. 2 and 3, even protonated pectin peels still contain several acidic sites. The maximum amount of metal bound (experimental data) was typically around 1 mequiv./g (Figs. 4–6), which is similar to the total number of binding sites for PPP (1.14 mequiv./g) but exceeds the number of carboxylate sites (0.39 mequiv./g), as listed in Table 1. This indicates that though carboxylate groups are important for metal binding in citrus peels, other sites might also play a role. Though it is plausible that conformational changes in pectin gel could occur, leading to auto-cooperative effects in metal binding, apparently this played a minor role in PPP since the metal binding followed a typical Langmuir behavior.

3.3. Comparison of different sorbent materials using Langmuir isotherms

As shown in Fig. 5, PPP showed an increase in sorption capacity compared to the material with the next highest capacity, non-protonated lemon peels. This can be attributed to two causes. The elimination of hard ions like Ca^{2+} and Mg^{2+} as a result of protonation increased the uptake of cadmium by reducing competition by those ions. The capacity also increased because PPP has an higher pectin content than the untreated lemon peel.

The Langmuir model was used to fit data in Figs. 4 and 5; values for K and q_{max} are listed in Table 2. Those parameters were obtained either by linearization or by minimizing the root mean square error (RMSE) between model and data. At both pH values, PPP (lemon based) were the best sorbent, followed by lemon and orange peels. This is evident by the trends in q_{max} and K values in Table 2.

Table 3
Parameters for pH-sensitive models with 1:1 and 1:2 stoichiometry for Cd binding by protonated pectin peels (PPP)

	Model type and method of parameter determination	K_{BM} (L/mequiv.)	B_T (mequiv./g)	RMSE
PPP, $CdCl_2$ pH 5	1:1 stoich, opti K and B_T	1.95	1.11	0.081
	1:1 stoich, opti K for pH 5	1.80	1.14[a]	0.081
	1:2 stoich, opti K and B_T	0.12	2.73	0.041
	1:2 stoich, opti K for pH 5	2.04	1.14[a]	0.092
PPP, Cd $(NO_3)_2$ SAM pH 5	1:1 stoich, opti K and B_T	4.14	1.19	0.031
	1:1 stoich, opti K for pH 3	4.36	1.14[a]	0.036
	1:1 stoich, opti K for pH 5	4.60	1.14[a]	0.034
	1:1 stoich, opti K for both pH	**4.48**	**1.14[a]**	**0.035**
	1:2 stoich, opti K and B_T	0.44	2.24	0.098
	1:2 stoich, opti K for pH 3	17.4	1.14[a]	0.240
	1:2 stoich, opti K for pH 5	**4.58**	**1.14[a]**	**0.165**
	1:2 stoich, opti K for both pH	**9.10**	**1.14[a]**	**0.188**
PPP, Cd $(NO_3)_2$ SAM pH 3	1:1 stoich, opti K and B_T	7.46	0.88	0.033
	1:1 stoich, opti K for pH 3	4.36	1.14[a]	0.047
	1:1 stoich, opti K for pH 5	4.60	1.14[a]	0.048
	1:1 stoich, opti K for both pH	**4.48**	**1.14[a]**	**0.048**
	1:2 stoich, opti K and B_T	0.034	16.47	0.060
	1:2 stoich, opti K for pH 3	**17.4**	**1.14[a]**	**0.085**
	1:2 stoich, opti K for pH 5	4.58	1.14[a]	0.158
	1:2 stoich, opti K for both pH	**9.10**	**1.14[a]**	**0.110**

Data were obtained with the sequential additions method (SAM) at pH 3 and 5, as well as the conventional method at pH 5. Parameters shown are the equilibrium metal binding constant K_{BM}, the number of binding sites B_T, and the root mean square errors (RMSE). Model versions shown in bold are depicted in Fig. 6.
[a] Total number of sites as determined from titration.

3.4. Langmuir isotherms at different pH

At pH 5 the uptake capacity was consistently higher than at pH 3, as is apparent from the orange peel sorption isotherm in Fig. 4 and the isotherm for PPP in Fig. 6. Similar results were observed for lemon and grapefruit peels [18]. The maximum apparent uptake capacity according to the Langmuir model was consistently lower at pH 3 than at pH 5 (Table 2). However, this is only an artifact of the Langmuir model. The reason for lower metal binding at pH 3 was an increased concentration of protons, which acted as a competitor, lowering the amount of sites available for metal binding, as described by Schiewer and Volesky [3] for carboxylate groups in algal biomass. If the same number of sites (1.14 mequiv./g) is assumed for both pH values, lower K values are obtained for pH 3. This can be explained using Eq. (25), where the apparent binding constant $K = K_{BM}/(1 + [H^+]/K_a)$. For $pH < pK_a$, the apparent binding constant would therefore be reduced. It would therefore be most appropriate to use a pH-sensitive model that takes changing site availability as a function of pH into account.

3.5. Developing pH-sensitive isotherms

The pH-sensitive isotherms with 1:2 or 1:1 stoichiometry (Eqs. (21) and (24)) were used to fit experimental SAM data. The unknown parameters K and B_T were determined by minimizing the RMSE between the model and experimental data. To prevent instability of the numerical solution, only one binding site was considered, and the proton binding constant (K_{CH}) for this site was assumed to be $10^{3.8}$, as determined for the main binding site (carboxylate). However, since the actual metal binding may involve several sites, the site quantity was adjusted to fit the experimental data rather than assuming only the carboxylate site quantity obtained from titrations. Table 3 shows model parameters for the pH-sensitive models. Obviously the best fits (lowest RMSE) are obtained if both K_{BM} and B_T are optimized for the particular isotherm (top row for each model type). For the 1:1 stoichiometry, the optimum B_T and RMSE were identical to those of the Langmuir model (Table 2), with only the binding constants differing. This is the case because, as explained in Eq. (26), for constant pH the 1:1 stoichiometry reduces to the Langmuir model with $K = K_{BM}/(1 + [H^+]/K_a)$.

The optimized B_T values for the 1:1 stoichiometry were similar to the total number of sites obtained by titration $B_T = 1.14$ mequiv./g (see Table 1), indicating that other sites in addition to carboxylate groups may be involved in metal binding. Therefore, Table 3 also lists equilibrium constants that were optimized assuming $B_T = 1.14$ mequiv./g. Good predictions were still obtained, especially for the 1:1 stoichiometry, when only K was optimized to fit the individual isotherm.

Theoretically, for pH-sensitive isotherms, one equilibrium constant should be valid for different pH values. Therefore, Table 3 also indicates the performance of the model (for the SAM method with $B_T = 1.14$ mequiv./g) if K was optimized for one pH value and used to predict data for the other pH value, or if one K value was optimized to fit data at both pH values. It is apparent that the 1:1 model fits virtually equally good in either case, which means that the model can truly predict the effect of pH using the K value obtained by fitting data obtained at one pH to predict the performance at a different pH. For the 1:2 stoichiometry model, predicting the pH is also possible but with a slightly larger error.

3.6. Comparison of 1:1 and 1:2 stoichiometry

With one exception (optimized K and B_T for conventional method), the model predictions of the 1:1 stoichiometry were superior and had lower RMSE (0.031–0.081 mequiv./g, corresponding to 3–7% of B_T) than those of the 1:2 stoichiometry, which had higher RMSE (0.041–0.098 mequiv./g, corresponding to 2–14% of B_T). This is also apparent in Fig. 6, which shows the model predictions of both types of pH-sensitive isotherm models for pH 3 and 5. The same value ($K = 4.48$ for 1:1 stoichiometry, $K = 9.10$ for 1:2 stoichiometry) was used for both pH values, showing that it is indeed possible to predict pH effects. To depict the data at low concentrations more clearly, the isotherm is plotted on a logarithmic scale. It should be noted that if plotted on a linear scale, these data do not follow a "half bell shape" but show a standard Langmuir behavior. The 1:2 stoichiometry under-predicts metal binding at high concentrations and over-predicts at low concentrations (which is only apparent when the concentration is plotted in a logarithmic scale, as done in Fig. 6), and generally features a more gradual increase, whereas the 1:1 stoichiometry fits the behavior of the data exactly. This behavior was unexpected since previous research had shown that the 1:2 stoichiometry was performing well for divalent metal ions (Cu and Ni) binding to carboxylate groups in seaweeds [27].

The question arises as to how the 1:1 stoichiometry can be explained mechanistically for divalent ions. Our observation that the 1:1 stoichiometry fits could be interpreted such that each metal ion binds to one site through chemical sorption (covalent binding/complexation), so that, from a reaction chemistry standpoint, the rate is first order with respect to the site concentration and the metal concentration. Nevertheless, only a maximum of one mole of a divalent ion can be bound by two moles of monovalent binding sites, indicating that secondary physical interactions such as electrostatic attraction to a second group may play a role. Another possible interpretation would be that a divalent metal simply binds to a monovalent site, whereby only half of the total number of sites determined in titrations actually participate in metal binding. This could be the sites contributing to the base charge already present at pH 2.6, plus Site 1, which together account for 0.59 mmol/g. If one divalent metal bound to each of those sites, a maximum cadmium uptake capacity of 1.18 mequiv./g would be expected, which again matches the experimental data. Based on the present experimental data, it cannot be concluded which of these interpretations is mechanistically correct, but the results support that binding of divalent metal ions can deviate from the expected 1:2 stoichiometry.

Acknowledgements

Funding by an EPSCoR graduate fellowship for S. Patil and an EPSCoR start up grant for S. Schiewer is gratefully acknowledged. The authors thank Sunkist Corporation for donating pectin peels. Thanks also to Dr. Smith (Wilfried Laurier University, Canada) for providing information about the FOCUS model.

References

[1] T. Davis, B. Volesky, A. Mucci, A review of the biochemistry of heavy metal biosorption by brown algae, Water Res. 37 (2003) 4311–4330.
[2] E. Fourest, B. Volesky, Contribution of sulphonate groups and alginate to heavy metal biosorption by the dry biomass of *Sargassum fluitans*, Environ. Sci. Technol. 30 (1996) 277–282.
[3] S. Schiewer, B. Volesky, Modeling of the proton-metal ion exchange in biosorption, Environ. Sci. Technol. 29 (1995) 3049–3058.
[4] V.M. Dronnet, C.M.G.C. Renard, M.A.V. Axelos, J.F. Thibault, Characterization and selectivity of divalent metal ion binding by citrus and sugar beet pectin, Carbohydr. Polym. 30 (1996) 253–263.
[5] C.M.G.C. Renard, M.C. Jarvis, Acetylation and methylation of homogalacturans 2: effect on ion-binding properties and conformations, Carbohydr. Polym. 39 (1999) 209–216.
[6] V.M. Dronnet, C.M.G.C. Renard, M.A.V. Axelos, J.F. Thibault, Binding of divalent metal cations by sugar-beet pulp, Carbohydr. Polym. 34 (1/2) (1997) 73–82.
[7] Z. Reddad, C. Gerente, Y. Andres, P. Le Cloirec, Modeling of single and competitive metal adsorption onto a natural polysaccharide, Environ. Sci. Technol. 36 (10) (2002) 2242–2248.
[8] S. Senthilkumaar, S. Bharathi, D. Nithayanadhi, V. Suburam, Biosorption of toxic heavy metals from aqueous solutions, Bioresour. Technol. 75 (2) (2000) 163–165.
[9] M. Ajmal, R.A. Khan-Rao, R. Ahmad, J. Ahmad, Adsorption studies of *Citrus reticulata* (fruit peel of orange): removal of Ni(II) from electroplating wastewater, J. Hazard. Mater. 79 (1/2) (2000) 117–131.
[10] S.H. Lee, S.J. Shon, H. Chung, M.-Y. Lee, J.-W. Yang, Effect of chemical modification of carboxylate groups in apple residues on metal ion binding, Korean J. Chem. Eng. 16 (1999) 576–580.
[11] E. Maranon, H. Sastre, Behavior of lignocellulosic apple residues in the sorption of trace metals in packed beds, React. Polym. 18 (1992) 173–176.
[12] G. Annadurai, R.S. Juang, D.J. Lee, Adsorption of heavy metals from water using banana and orange peels, Water Sci. Technol. 47 (2003) 185–190.
[13] R. Jumle, M.L. Narwade, U. Wasnik, Studies in adsorption of some toxic metal ions on *Citrus sinesis* skin and *Coffea arabica* husk: agricultural byproduct, Asian J. Chem. 14 (2002) 1257–1260.
[14] P. Harel, L. Mignot, J.P. Sauvage, G.P. Junter, Cadmium removal from dilute aqueous solution by gel beads of sugar beet pectin, Ind. Crops Prod. 7 (1998) 239–247.
[15] M.T. Kartel, L.A. Kupchik, B.K. Veisov, Evaluation of pectin binding of heavy metal ions in aqueous solutions, Chemosphere 38 (1999) 2591–2596.
[16] R. Kohn, Binding of divalent cations to oligomeric fragments of pectin, Carbohydr. Res. 160 (1987) 343–353.
[17] P. Lodeiro, R. Herrero, M.E. Sastre de Vincente, Thermodynamic and kinetic aspects on the biosorption of cadmium by low cost materials: a review, Environ. Chem. 3 (2006) 400–418.
[18] S. Schiewer, S. Patil, Pectin-rich fruit wastes as biosorbents for heavy metal removal: Equilibrium and kinetics, Bioresource Technol. 99 (6) (2008) 1896–1903.
[19] X.M. Li, Y.R. Tang, Z.X. Xuan, Y.H. Liu, F. Luo, Study on the preparation of orange peel cellulose adsorbents and biosorption of Cd from aqueous solution, Sep. Purif. Technol. 55 (1) (2007) 69–75.
[20] Z. Xuan, Y. Tang, X. Li, Y. Liu, F. Luo, Study on the equilibrium, kinetics and isotherm of biosorption of lead ions onto pretreated chemically modified orange peel, Biochem. Eng. J. 31 (2006) 160–164.
[21] A.B. Perez-Marin, V. Meseguer Zapata, J.F. Ortuno, M. Aguilar, J. Saez, M. Llorens, Removal of cadmium from aqueous solutions by adsorption onto orange waste, J. Hazard. Mater. B139 (2007) 122–131.
[22] M. Cernik, M. Borkovec, J.C. Westall, Regularized least-squares methods for the calculations of discrete and continuous affinity distributions for heterogeneous sorbents, Environ. Sci. Technol. 29 (1995) 413–415.
[23] S.D. Smith, G.F. Ferris, Proton binding by hydrous ferric oxide and aluminum oxide surfaces interpreted using fully optimized continuous pK_a spectra, Environ. Sci. Technol. 35 (23) (2001) 4637–4642.

[24] F. Pangnanelli, P.M. Papini, M. Toro, F. Veglio, Biosorption of metal ions on *Arthrobacter* sp.: biomass characterization and biosorption modeling, Environ. Sci. Technol. 33 (2000) 2773–2778.
[25] J. Buffle, Complexation of Reactions in Aquatic Systems—An Analytical Approach, Ellis Horward Limited, Chichester, UK, 1990.
[26] G.T. Grant, E.R. Morris, D.A. Rees, P.J.C. Smith, D. Thom, Biological interactions between polysaccharides and divalent cations: the egg-box model, FEBS Lett. 32 (1973) 195–198.
[27] S. Schiewer, M.H. Wong, Metal binding stoichiometry and isotherm choice in biosorption, Environ. Sci. Technol. 33 (1999) 3821–3828.